

Glutamatergic modulation of slow inward rectification in trigeminal primary sensory neurons

SUSUMU TANAKA, KOUICHI YASUDA and KIYOFUMI FURUSAWA

Department of Oral and Maxillofacial Surgery, School of Dentistry, Matsumoto Dental University

Summary

In the present study, we showed that activation of metabotropic glutamate receptors in rat mesencephalic trigeminal (Mes V) neurons (which are important in the genesis and control of oral-motor activities) can modulate hyperpolarization-activated inward current (I_h). Whole-cell recordings were obtained from rat Mes V neurons, and I_h was induced by a hyperpolarizing current or voltage pulses. Application of ACPD, which is a group I and II mGluRs agonist, suppressed the voltage- and time-dependent voltage sag under current-clamp recording, and suppressed the steady-state inward current under voltage-clamp recording, suggesting that it inhibited I_h . Further investigation revealed that group II mGluRs activation and the release of intracellular Ca^{2+} mediated ACPD-induced inhibition of I_h . Additionally, low-frequency (<10Hz) resonant properties exhibited at membrane potentials ranging from resting potential to hyperpolarization were substantially reduced by ACPD, indicating that modulation of I_h by mGluRs activation induces substantial changes in the frequency preference with which neurons respond to synaptic inputs.

Introduction

Mes V neurons are critically involved in the regulation of oral-motor activities. Their unique location within the brainstem is consistent with the role of sensory neurons or integrative interneurons, and they project axons to motoneurons and premotoneurons that control the jaw musculature^{1,2}). In a recent study, inward rectification manifesting as a depolarizing sag was prominent in Mes V neurons, suggesting that I_h (the slow inward rectifying conductance underlying this membrane property) contributes to the subthreshold and firing behavior of Mes V neurons³). The available evidence suggests that I_h activation at resting membrane potential and the presence of low-frequency resonance at potentials ranging from rest to hyperpolarization allow these neurons to fire not only at depolarized membrane potentials but also within the resonant frequency range, via amplification of the membrane drive potentials consisting of a hyperpolarizing component³).

Endogenously released neurotransmitters have been shown to modulate the firing characteristics and cell excitability of neurons via modulation of I_h conductances in other neuronal systems⁴). As for Mes V neurons, recent study demonstrated that the membrane excitability of Mes V neurons was regulated by 5-HT receptor activation via suppressive modulation of persistent sodium (I_{NaP}) con-

ductance⁵), which is critical for subthreshold voltage oscillations and high-frequency discharge of Mes V neurons^{6,7}). Despite such studies are essential for elucidating how various neuromessengers that are involved in modulation of ion conductances of Mes V neurons work in concert to modulate oral-motor activities, there have been no studies related to the modulation of I_h in Mes V neurons.

In a previous immunohistochemical study, metabotropic glutamate receptors (mGluRs) were found to be specifically expressed in trigeminal neurons, including Mes V neurons⁸). Research indicates that mGluRs on trigeminal motoneurons are involved in burst generation⁹ and regulation of intrinsic and synaptic properties¹⁰), but little is known about the role of mGluRs in the regulation of the ionic conductances and cellular excitability of Mes V neurons. Therefore, in the present study, we investigated the possibility that mGluRs are involved in modulation of I_h in Mes V neurons.

Material and Methods

Preparation of tissue slices

Coronal brainstem slices containing the mesencephalic trigeminal nucleus were prepared from tissue obtained from P 2–4 and P 9–12-day-old Sprague–Dawley rats, as described previously^{3,5–7}). Briefly, rats were handled according to the policy of The American Physiological Society regarding the use and care of animals. Rats were anesthetized by halothane inhalation, the brainstem was carefully removed and immersed in oxygenated ice-cold cutting solution of the following composition : 126mM NaCl, 3mM KCl, 1.25mM NaH₂PO₄, 26mM NaHCO₃, 10mM glucose, 1mM CaCl₂, 5 mM MgCl₂, and 4mM lactic acid¹¹). Coronal sections (thickness, 300μm) were cut with a microslicer (DSK Microslicer), incubated (40 min at 37°C), and immersed in oxygenated incubation solution at room temperature (22–24°C).

The composition of normal ACSF was as follows : 124mM NaCl, 3mM KCl, 1.25mM NaH₂PO₄, 26 mM NaHCO₃, 10mM glucose, 2mM CaCl₂, and 2mM MgCl₂. The incubation solution was created by adding 4mM lactic acid to normal ACSF. In voltage-clamp experiments, to isolate the slow inward rectifying current (I_h), the recording solution was replaced with various external solutions. The external solution for I_h was similar to that used in a previous study³), and contained the following : 114 mM NaCl, 3mM KCl, 26mM NaHCO₃, 10mM glucose, 1.5mM CaCl₂, 0.5mM BaCl₂, 2mM MgCl₂, 10 mM TEA-Cl, 0.1mM CdCl₂, 2mM 4-aminopyridine (4-AP), and 0.0005mM TTX. NaH₂PO₄ was omitted from the solution to avoid precipitation. All solutions were equilibrated with 95% O₂–5% CO₂, and the pH was adjusted to 7.3. The composition of the intrapipette solution was as follows : 115mM K-gluconate, 25mM KCl, 9mM NaCl, 10mM HEPES, 0.2mM EGTA, 1mM MgCl₂, 3mM K₂-ATP, and 1mM Na-GTP 1. The pH and osmolarity were adjusted to 7.3 and 280 to 290 mOsm, respectively.

Drugs were used to examine the effects on I_h properties and dissolved in distilled water or dimethyl sulfoxide (DMSO) as stock solutions. They were then applied via rapid perfusion after stabilization of the peak current amplitude at the following concentrations : 1S, 3R-ACPD (Sigma), 20 μM ; MCPG (Sigma), 1mM ; AIDA (Sigma), 300μM ; EGLU (Tocris), 300μM ; DHPG (Sigma), 20 μM ; L-CCG-I (Calbiochem), 20μM ; BAPTA-AM (Sigma), 50μM. The drugs were bath-applied in the presence of bicuculline (10μM ; Sigma), strychnine (10μM ; Sigma), DNQX (10μM ; Sigma) and APV (10μM ; Sigma) to block inhibitory and excitatory ionotropic receptors¹⁰).

Patch-clamp recordings

Slow inward rectifying currents (I_h) were recorded using the patch-clamp technique in the whole-

cell configuration, using an Axopatch-1D patch-clamp amplifier and pCLAMP acquisition software (Axon instruments, Foster City, CA). Patch-electrodes (tip resistance, 2.5–3.5M Ω) were fabricated from thick-walled borosilicate glass (OD, 1.5mm ; ID, 0.86mm) (Sutter Instruments P-97, Novato, CA). Mes V neurons were easily identified by their pseudounipolar soma, using visual control with infrared differential interference contrast video microscopy, as described elsewhere^{8,5-7}. All signals were grounded using a 3M KCl–agar bridge electrode (Ag–AgCl wire), and were filtered using a low-pass Bessel filter at 5kHz. Uncompensated series resistance (Rs), which was less than 15M Ω , was compensated by 40 to 80% and monitored periodically during the experiments. Liquid junction potentials between bath and pipette solutions for isolation of fast or slow Na currents were approximately –5mV, and were corrected off-line¹².

Data analysis

Voltage and current signals were digitized and recorded using pCLAMP acquisition software (v 8.1, Axon Instruments) for subsequent analysis. In the voltage-clamp experiments, for I_h activation, the holding potential was initially –55mV, and was hyperpolarized to –140mV using a series of 5– to 10–mV voltage step commands as previously reported³. In the current-clamp experiments, to determine the effects of each drug on membrane properties, the membrane potential was maintained at the value of the control conditions, by application of extrinsic current via the recording pipette.

For frequency-domain analysis, a ZAP input current at frequencies ranging from 0 to 250Hz was injected into neurons, and the membrane voltage responses were recorded as described elsewhere^{13,14}. We used a low-pass filter at 0.5kHz to reduce the noise of the input current. The current and voltage records were digitized at a frequency of 10kHz. Impedance (Z) was calculated from the ratio of the Fast Fourier transforms (FFT) of the voltage response and the input current, using the following formula : $Z = \text{FFT}(V) / \text{FFT}(I)$.

The frequency-response curve (FRC) was obtained by plotting frequency against the magnitude of impedance. When resonant behavior was detected, the resonant frequency (F_{res}) and the Q value were measured. The F_{res} was defined as the frequency at the peak of the hump in the FRC. The Q value was calculated by measuring the impedance at F_{res} and dividing that value by the magnitude of the impedance at the lowest frequency measured^{7,15,16}.

Data analysis was performed using a combination of software : StatView (SAS Institute, Cary, NC), Sigmaplot 4.0 (Jandel Scientific, San Rafael, CA), Datapac III (v1.61 ; Run Technologies, Irvine, CA), and Microsoft Excel. Results were reported as mean \pm SE (standard error). The significance of differences between means was assessed using Student's *t* test. A probability value of $p < 0.05$ was considered to indicate statistical significance, unless otherwise stated.

Results

To avoid sampling bias, the present results were obtained from rat Mes V neurons throughout the rostral-caudal extent of the mesencephalic trigeminal nucleus. After establishing the whole-cell configuration, cells were held at a membrane potential of –65mV in normal ACSF. Then, a hyperpolarization-activated slow inward current (I_h) was induced in cells in modified ACSF (see Methods). In most cells, I_h exhibited a decrease associated with the decrease in peak maximal amplitude and the shift of the activation curve to more hyperpolarized potentials ; the same phenomenon has previously been observed for other types of neurons¹⁷. The time course and extent of the decrease in I_h varied among cells. We periodically monitored the series resistance and peak amplitude of I_h. Subse-

quent recordings were performed only when the series resistance was relatively small ($<10\text{M}\Omega$) and there was a small change in the decrease in the peak amplitude of I_h before drug application ($<10\%$).

ACPD reduces I_h in Mes V neurons.

Figure 1A is a voltage–current (V–I) curve in which the voltage response is plotted as a function of hyperpolarizing current pulse. In current–clamp recording in normal ACSF, the hyperpolarizing current pulse exhibited a robust voltage– and time–dependent depolarizing sag, due to the activation of I_h ; this phenomenon has previously been reported for other types of neurons⁹. The difference between the peak and steady–state voltage responses indicates the magnitude of I_h . Application of 1 S, 3R–ACPD (ACPD ; $20\mu\text{M}$) significantly slowed the voltage response and reduced the difference between the peak and steady–state voltage responses (mean % reduction of voltage sag, $11.2 \pm 2.0\%$; $n = 5$), indicating that I_h is negatively modulated by mGluR activation (Fig. 1A). Therefore, we performed a series of voltage–clamp experiments to investigate the effects of ACPD on I_h characteristics. Figure 1B shows a representative current trace from a P10 Mes V neuron in response to hyperpolarization from the holding potential (-55mV) to -140mV . The instantaneous current (*) was measured immediately after the decay of the capacitive transient. The steady–state current (**) developed slowly, and was measured near the end of the voltage command. In the presence of ACPD, the steady–state current was substantially decreased, compared with the control. The effect of ACPD on the instantaneous current was small, and the difference between the instantaneous and steady–state currents (representing I_h amplitude) was significantly reduced by ACPD. The effect of

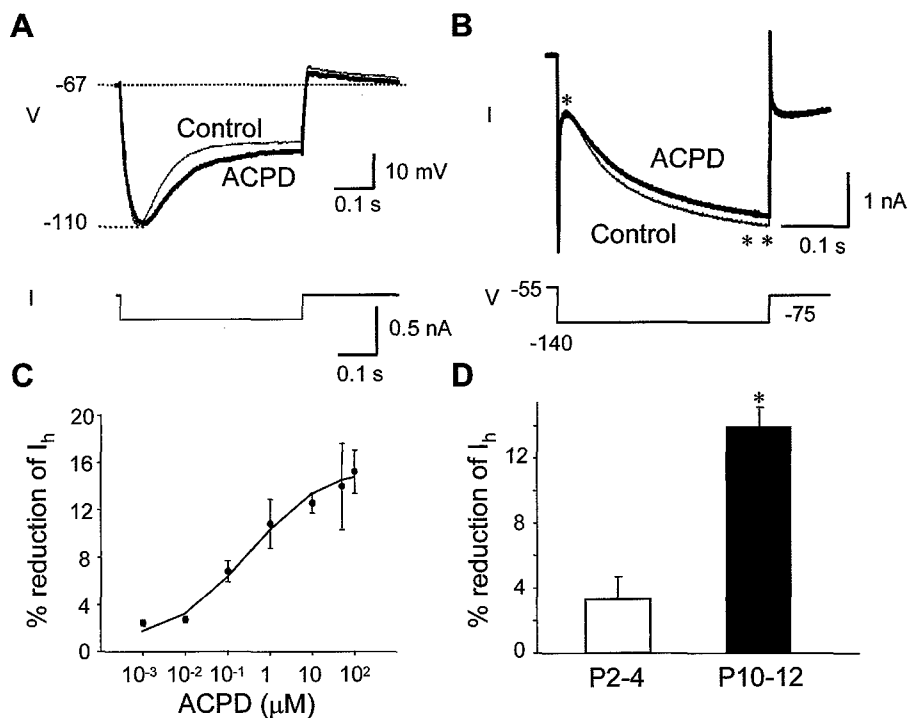


Figure 1 : mGluRs activation modulates I_h in Mes V neurons. A : The voltage response evoked by hyperpolarizing current pulse reached a peak (-110mV), followed by depolarizing sag in P11 neuron. Application of ACPD ($20\mu\text{M}$) decreased the amplitude of the sag, indicating inhibition of I_h . B : A representative current trace from another neuron evoked by hyperpolarizing voltage step changing the membrane potential from a holding potential of -55mV to -140mV . ACPD substantially decreased the steady–state current, but had little effect on the instantaneous current. C : ACPD decreased the difference between the instantaneous and steady–state currents (I_h amplitude) in a concentration–dependent manner. D : The ACPD–induced decrease in I_h was developmentally regulated. *, significant difference between older neurons (P10–12, $n = 10$) and younger neurons (P2–4, $n = 8$) ($p < 0.05$).

ACPD on I_h increased as the concentration of ACPD increased (Fig. 1C). Also the mean % reduction of I_h amplitude was greater in older neurons (P10–12, $13.8 \pm 1.1\%$; $n = 10$) than in younger neurons (P 2–4, $3.3 \pm 1.9\%$; $n = 8$), suggesting postnatal development of the modulatory effect of mGluR activation on I_h (Fig. 1D). Therefore, we used P10–12 neurons in the following experiments.

The effects of ACPD on I_h activation characteristics

The decrease in I_h amplitude could be due to the decrease in maximal I_h conductance, a shift of the gating properties of I_h activation, or both. To quantify the effect of ACPD on I_h activation, the older (P10–12) neurons were subjected to a series of hyperpolarizing command voltage steps that changed the membrane potential from a holding potential of -55mV to a membrane potential of -140 to -60mV (Fig. 2A). Tail currents evoked after the membrane potential returned to -75mV were normalized as previously reported³⁾. As shown in Fig. 2B, the voltage-dependent activation plots of I_h fit well with the Boltzmann equation in the following form: $I/I_{\text{max}} = 1 / \{1 + \exp(V_{1/2} - V)/k\}$ (I_{max} , maximal peak current; V , applied step command potential; $V_{1/2}$, half maximal activation voltage; k , slope factor). We observed small but statistically significant hyperpolarizing shifts with half-maximal activation by ACPD (control, $-106.9 \pm 1.1\text{mV}$; ACPD, $-108.6 \pm 1.2\text{mV}$; $n = 5$; $p < 0.05$). The I_h conductance (G_h) was calculated using the following equation: $G_h = I_h / (V - E_{\text{rev}})$, where V is applied command potential, I_h is the peak amplitude, and E_{rev} is the measured reversal potential of -40mV under the experimental conditions. As shown in Fig. 2C, G_h (measured at peak amplitude) was substantially decreased by ACPD (control, $23.8 \pm 1.4\text{pS}$; ACPD, $18.2 \pm 1.6\text{pS}$; $n = 5$; $p < 0.05$).

The effect of ACPD on the activation kinetics was further examined using a hyperpolarizing long step (5s) protocol. The voltage-dependent time course of I_h activation was fitted with 2 time con-

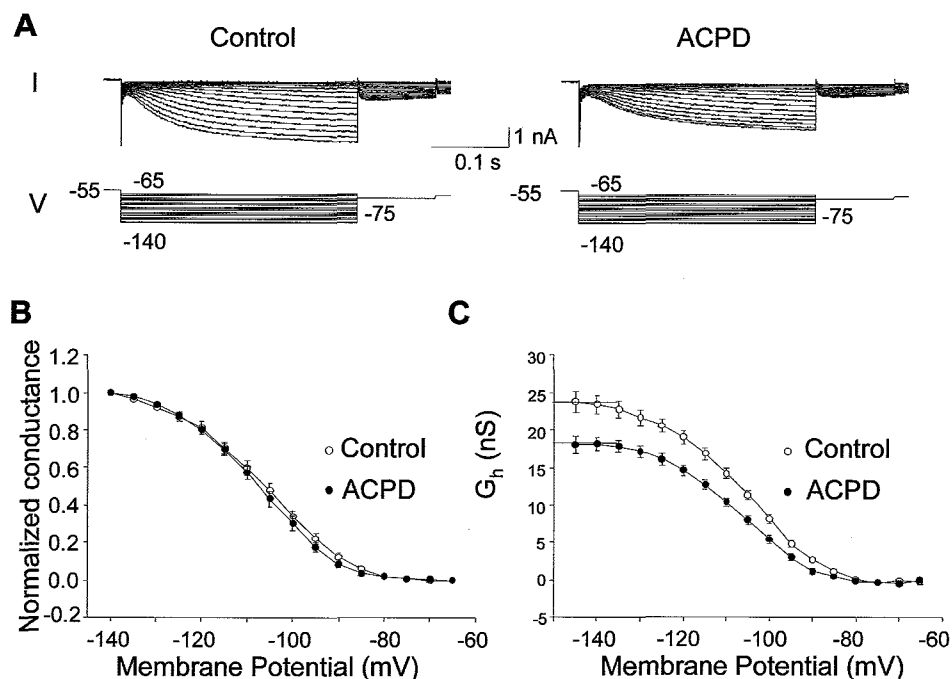


Figure 2: Suppression of I_h by mGluRs activation is mediated by a decrease in $G_{h\text{max}}$. A: Current responses evoked by hyperpolarizing voltage steps changing the membrane potential from a holding potential of -55mV to hyperpolarized potentials ranging from -140 to -65mV , before and after application of ACPD. Tail currents were observed at -75mV after termination of pulse. B: Boltzmann fits of the activation curves for controls (open circles) and in the presence of ACPD (closed circles), based on tail current analysis. Half-activation value was not shifted by ACPD. C: Application of ACPD significantly reduced the maximal I_h conductance ($G_{h\text{max}}$).

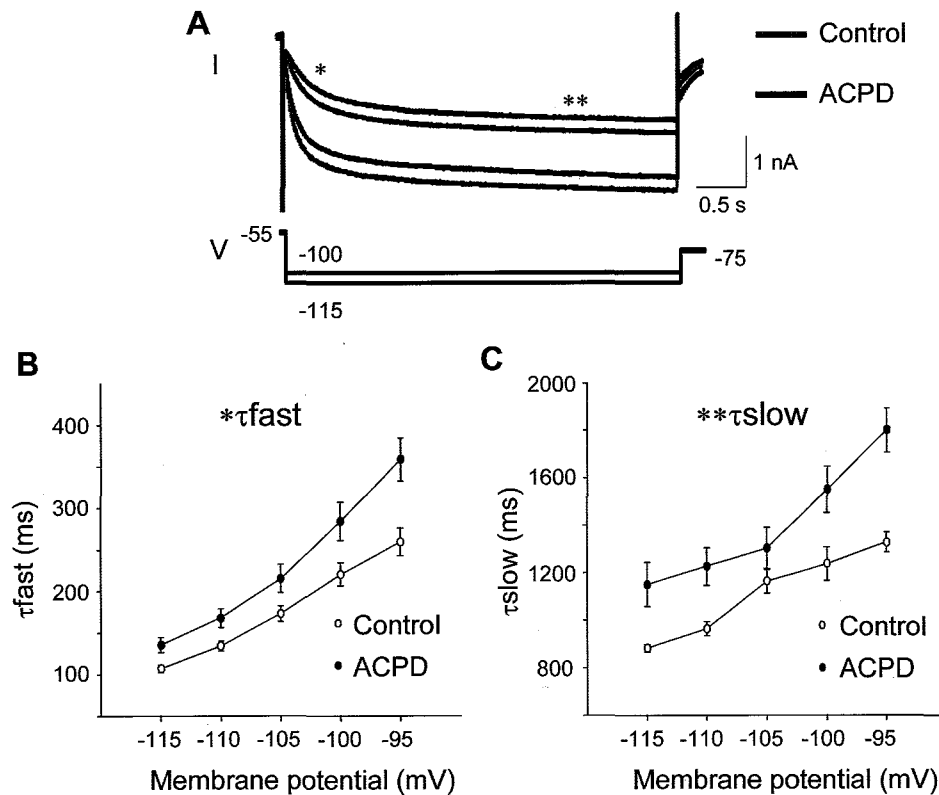


Figure 3 : The effects of mGluRs activation on I_h activation kinetics. A : The activation time course of I_h evoked by long (5s) hyperpolarizing step (-115 and -100 mV) protocol before and after application of ACPD was a good fit for the double exponential time constants. B : Composite plot of fast and slow time constants for I_h activation as a function of voltage before and after application of ACPD. ACPD slowed both fast and slow time constants at all hyperpolarizing voltage commands.

stants under normal conditions, as previously reported³). Application of ACPD significantly slowed both fast (τ_{fast}) and slow (τ_{slow}) time constants at all hyperpolarizing membrane potentials ($V_m = -105$ mV : τ_{fast} control, 170 ± 1.6 ms ; τ_{fast} ACPD, 210 ± 2.9 ms ; τ_{slow} control, 1160 ± 1.7 ms ; τ_{slow} ACPD, 1290 ± 2.5 ms ; $n = 5$; $p < 0.05$) (Fig. 3A and B).

Involvement of group II mGluR receptor activation and release of intracellular Ca^{2+} in ACPD-induced inhibition of I_h

ACPD activates multiple mGluR subtypes, and it is unclear which subtypes are involved in suppressive modulation of I_h . To characterize pharmacologically the specific types of mGluRs^{18,19} that underlie ACPD-induced modulation of I_h in Mes V neurons, we analyzed the effects of various agonists and antagonists of mGluRs on I_h in another subset of neurons. Figure 4 shows the histogram representing the mean change in I_h amplitude after application of each agonist and antagonist. As shown in Fig. 4A, MCPG (1 mM), which is a specific antagonist of group I and II mGluRs, completely blocked ACPD-induced suppression of I_h (mean % reduction, $1.6 \pm 1.3\%$; $n = 4$; $p < 0.05$). After pre-incubation with AIDA (300 μ M), which is a specific antagonist of group I mGluRs, ACPD induced a modest decrease in the amplitude of I_h (mean reduction, $6.3 \pm 0.8\%$; $n = 5$; $p = 0.23$). In contrast, EGLU (300 μ M), which is a specific antagonist of group II mGluRs, antagonized the effect of ACPD on I_h (mean reduction, $2.5 \pm 1.5\%$; $n = 5$; $p < 0.05$). In further experiments, DHPG (20 μ M), which is a specific agonist of group I mGluRs, induced a minor decrease in I_h amplitude (mean reduction, $3.5 \pm 1.7\%$; $n = 6$; $p < 0.05$), and L-CCG-I (20 μ M), which is a specific agonist of group II mGluRs, mim-

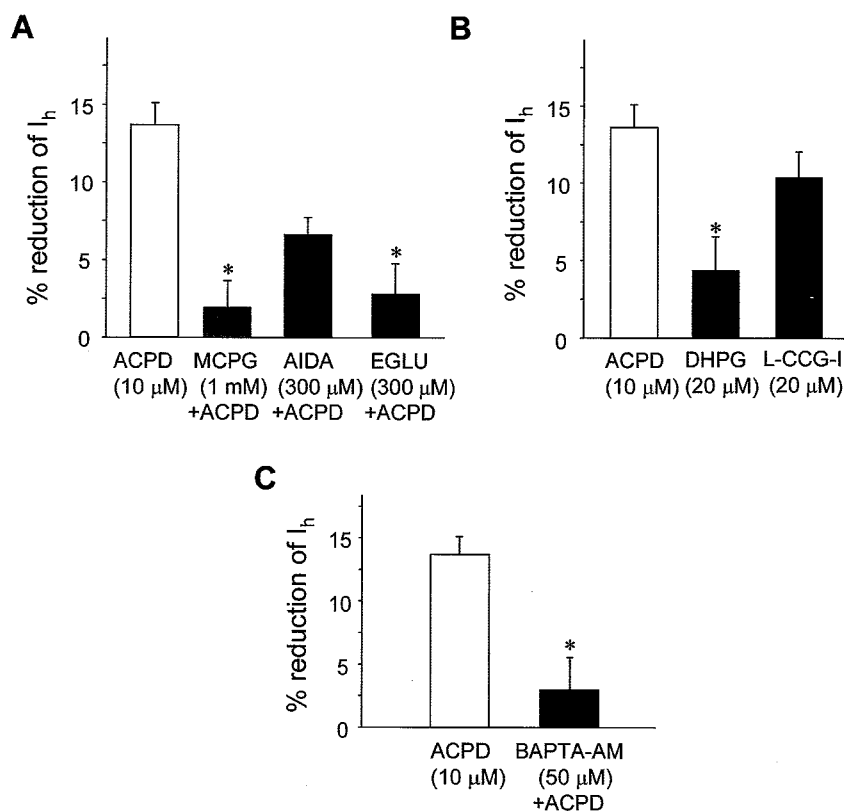


Figure 4: Group II mGluRs activation and release of intracellular Ca^{2+} mediate ACPD-induced inhibition of I_h . A, B: Bars indicate the mean percent reduction of I_h amplitude measured at -140 mV in the presence of agonists or antagonists of mGluRs. Both MCPG (300–500 μ M) and EGLU (300 μ M) significantly blocked the ACPD-induced reduction of I_h (A). L-CCG-I (20 μ M) mimicked the effect of ACPD on I_h , but DHPG (20 μ M) did not. C: Intracellular Ca^{2+} chelators (BAPTA-AM, 50 μ M), significantly blocked ACPD-induced suppression of I_h . *, significantly different from data for ACPD ($p < 0.05$).

icked the effect of ACPD on I_h (mean reduction, $10.2 \pm 1.3\%$; $n = 7$; $p = 0.57$) (Fig. 4B).

Studies indicate that the intracellular Ca^{2+} concentration is involved in modulation of I_h or modulation of other voltage-gated currents by various neurotransmitters in neurons other than Mes V neurons^{20–22}. Therefore, we further examined the effect of a Ca^{2+} chelator to test whether ACPD-induced reduction of I_h could be modulated by effects on the intracellular Ca^{2+} concentration. We monitored the peak amplitude of I_h after preincubation of BAPTA-AM (50 μ M), a membrane-permeable intracellular Ca^{2+} chelator. BAPTA-AM, by itself, showed a modest decrease in the peak amplitude of I_h (5–7%). We then applied ACPD when the peak amplitude was stabilized. As shown in Fig. 4C, in the presence of extracellular BAPTA-AM (50 μ M), the effect of ACPD on the I_h amplitude was significantly reduced (mean reduction, $2.8 \pm 2.0\%$; $n = 5$).

Effects of mGluRs activation on resonant behavior

In a recent study³, Mes V neurons exhibited a low-frequency resonance (< 10 Hz) at voltages more negative than the resting potential, allowing them to discriminate between synaptic inputs on the basis of frequency content. This phenomenon is apparently mediated by I_h activation. Therefore, to test whether mGluRs activation suppresses resonance via an inhibitory effect on I_h , we examined the effect of ACPD on resonance using frequency domain analysis. Fig. 5A shows representative examples of the impedance-frequency relationship in response to ZAP input currents at hyperpolarizing holding potentials of -70 to -80 mV. Bath application of ACPD (20 μ M) significantly suppressed

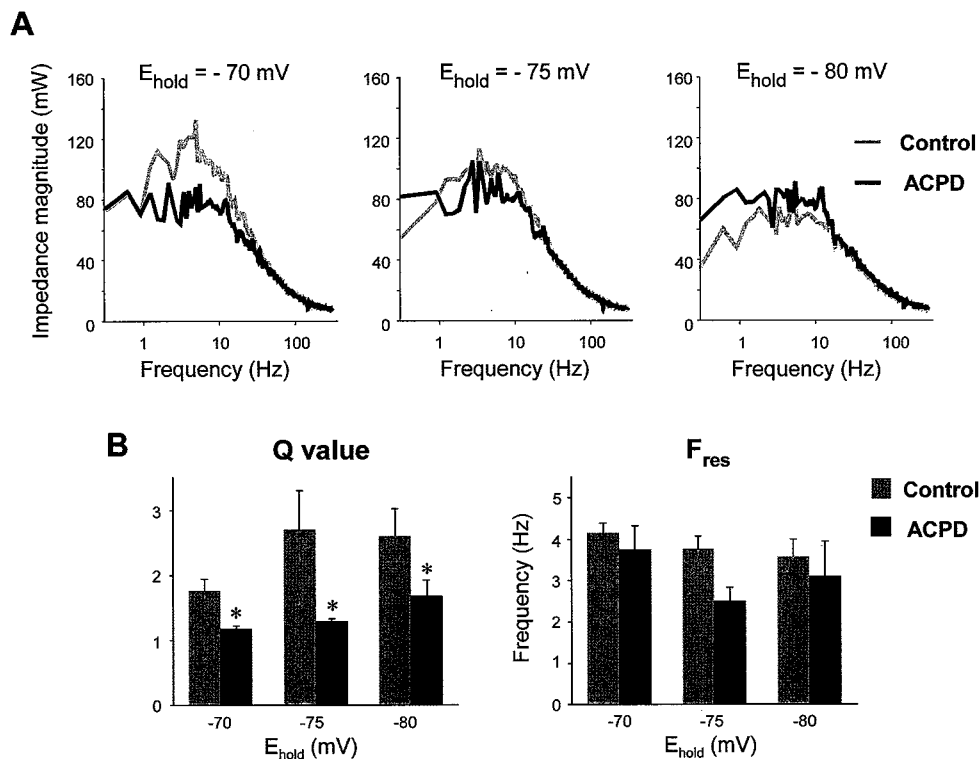


Figure 5 : mGluRs activation modulates low-frequency resonance in Mes V neurons. A : Frequency-domain analysis showed that ACPD significantly decreased the overall impedance magnitude of the frequency response curve (FRC) at holding potentials (E_{hold}) of -70 to -80 mV. B : Summary of Q-value and resonant frequency (F_{res}) before and after application of ACPD as a function of E_{hold} . *, significantly different from data for control conditions at the same E_{hold} . ($p < 0.05$).

the resonant peak, with significant reduction of the Q-value and little change in the resonant frequency (F_{res}) in most cells at the same holding potentials ($E_{\text{hold}} = -75$ mV : control Q-value, 1.75 ± 0.9 ; ACPD Q-value, 1.20 ± 0.3 ; $n = 5$; $p < 0.05$; control F_{res} , 4.18 ± 0.3 Hz ; ACPD F_{res} , 3.80 ± 0.8 Hz ; $n = 5$; $p = 0.95$) (Fig. 5B).

Discussion

The present study is the first detailed analysis of neurotransmitter-mediated modulation of I_h (hyperpolarization-activated inward current) in Mes V neurons. The present voltage-clamp experiments demonstrate that mGluRs activation suppresses the amplitude of I_h in Mes V neurons. This effect is dose-dependent and developmentally regulated. In conjunction with the developmental increase in current density of I_h ³⁾, despite the increase in soma size, differential immunoreactivity of mGluRs during postnatal development appears to contribute to the developmental change in ACPD-induced modulation of I_h in Mes V neurons. Since Mes V neurons demonstrate the developmental complexity in the spike discharge characteristics such as repetitive spike discharge and intrinsic bursting activities after postnatal day 6⁷⁾, we focused on clarifying the basic properties and the neuromodulation of ionic conductances underlying those activities in the following experiments. For this purpose, we closely examined the aspects of I_h modulation by mGluRs activation using older aged (P10–12) neurons.

In the present study, although the activation time constants and the kinetics of I_h were slowed by mGluRs activation, there was no significant shift in the activation curve (only a decrease in maximal conductance was observed). These results suggest that ACPD decreased the current density of active

I_h -channels, rather than changing their gating properties. As well as Mes V neurons, dorsal root ganglion (DRG) neurons also function as primary sensory neurons. DRG neurons, however, consist of different types of neurons and show heterogeneous expression of I_h ²³ in contrast to neonatal rat Mes V neurons³. Although the modulatory effects of mGluRs activation on I_h properties have not been clarified in these neurons, past studies revealed that serotonergic activation has excitatory effects on I_h in DRG neurons²³, as opposed to the inhibitory effects in Mes V neurons⁵.

Involvement of group II mGluR receptor activation and release of intracellular Ca^{2+} in ACPD-induced inhibition of I_h

In the present study, the effects of ACPD on I_h were specifically blocked by MCPG, indicating that these effects are nonspecific. Also, the effects of ACPD were mimicked by the group II-specific mGluR agonist L-CCG-I, and were significantly blocked by the group II-specific mGluR antagonist EGLU. Although we do not preclude the possibility that group I mGluRs play a role in modulation of I_h , it appears that modulation of I_h by ACPD is mainly mediated by group II mGluRs. This is not to suggest that all effects of mGluRs activation on membrane properties of Mes V neurons are mediated by group II mGluRs, because the group III-specific mGluR agonist L-AP4 (20 μ M) also reduced I_h (data not shown). These results are consistent with a previous immunohistochemical study, in which immunoreactivity of group I, II and III mGluRs was observed in the mesencephalic trigeminal nucleus of rats after postnatal day 3⁸.

In addition, the present study indicate that a minimum concentration of internal Ca^{2+} is required for normal expression of I_h like cat neocortical neurons²⁰ and ACPD-induced suppression of I_h is reduced by a chelation of internal Ca^{2+} . Although internal Ca^{2+} also has indirect effects on activity of cAMP and PKA²⁴, Ca^{2+} mobilization is supposed to play an important role in ACPD-induced modulation of I_h in Mes V neurons.

Functional implications of ACPD-dependent modulation of membrane excitability in Mes V neurons.

Mes V neurons, which are important interneurons due to their unique location in the brainstem, are critically involved in rhythmical oral motor activities. As previously demonstrated, I_h conductance contribute to membrane excitability of Mes V neurons by regulating spike discharge characteristics and producing resonant properties at membrane potentials ranging from resting potential to hyperpolarization⁹. In particular, resonance would be useful for rapid synchronization and stabilization of coordinated activity within the network. In the present current-clamp study, ACPD significantly reduced the frequency-current relationship and Q-value, which is consistent with a decrease in I_h . In contrast, the resonant frequency (which determines the spike frequency during the spike train or bursting activities) showed a smaller shift after ACPD application, compared to the shift observed in the modulation of high-frequency resonance by 5-HT.

Many previous *in vitro* studies have implicated endogenously glutamatergic neurotransmission via ionotropic receptors in generation of fictive mastication²⁵ and rhythmical trigeminal motor output involving central pattern generation²⁶. In contrast, endogenous mGluRs activation is not critically involved in generation of rhythmical jaw movements, and research suggests that trigeminal motoneurons exert a modulatory effect on synaptic membrane properties via pre- or post-synaptic suppression of synaptic transmission between premotoneurons and trigeminal motoneurons¹⁰. In addition, monosynaptic excitatory postsynaptic potentials (EPSPs) could be evoked in trigeminal

motoneurons by focal stimulation of the Mes V nucleus²⁷⁾. Together, these findings suggest that modulation of I_h by mGluRs activation could alter the resonant properties of Mes V neurons, thus changing the frequency preference with which Mes V neurons respond to synaptic inputs. Such changes may contribute to alteration of motoneuronal excitability and presynaptic alteration of signal transmission to trigeminal motoneurons.

Because many other intrinsic neurotransmitters act on the Mes V nucleus, further study is needed to determine how the effects of various neurotransmitters and neuromodulators on intrinsic and synaptic membrane properties of Mes V neurons are integrated, especially in certain forms of oral-motor dysfunction.

References

- 1) Luo P, Wong R and Dessem D (1995) Projection of jaw-muscle spindle afferents to the caudal brain stem in rats demonstrated using intracellular biotinamide. *J Comp Neurol* **358** : 63–78.
- 2) Dessem D and Taylor A (1989) Morphology of jaw-muscle spindle afferents in the rat. *J Comp Neurol* **282** : 389–403.
- 3) Tanaka S, Wu N, Hsiao CF, Turman J and Chandler SH (2003) Development of inward rectification and control of membrane excitability in mesencephalic V neurons. *J Neurophysiol* **89** : 1288–98.
- 4) Pape HC (1996) Queer current and pacemaker : The hyperpolarization-activated cation current in neurons. *Annu Rev Physiol* **58** : 299–327.
- 5) Tanaka S and Chandler SH (2006) Serotonergic modulation of persistent sodium currents and membrane excitability via cyclic AMP-protein kinase A cascade in mesencephalic V neurons. *J Neurosci Res* **83** : 1362–72.
- 6) Wu N, Enomoto A, Tanaka S, Hsiao CF, Nykamp DQ, Izhikevich E and Chandler SH (2005) Persistent sodium currents in mesencephalic V neurons participate in burst generation and control of membrane excitability. *J Neurophysiol* **93** : 2710–22.
- 7) Wu N, Hsiao CF and Chandler SH (2001) Membrane resonance and subthreshold membrane oscillations in mesencephalic V neurons : participants in bursting generation. *J Neurosci* **21** : 3729–39.
- 8) Turman JE, Hiyama L, Castillo M and Chandler SH (2001) Expression of group I and II metabotropic glutamate receptors in trigeminal neurons during postnatal development. *Dev Neurosci* **23** : 41–54.
- 9) Krieger P, Grillner S and EI Manira A (1998) Endogenous activation of metabotropic glutamate receptors contributes to burst frequency regulation in the lamprey locomotor network. *Eur J Neurosci* **10** : 3333–42.
- 10) Del Negro CA and Chandler SH (1998) Regulation of intrinsic and synaptic properties of neonatal rat trigeminal motoneurons by metabotropic glutamate receptors. *J Neurosci* **18** : 9216–26.
- 11) Schurr A, West CA and Rigor BM (1988) Lactate-supported synaptic function in the rat hippocampal slice preparation. *Science* **240** : 1326–8.
- 12) Neher E (1992) Correction for liquid junction potentials in patch-clamp experiments. *Methods Enzymol* **207** : 123–31.
- 13) Puil E, Gimbarzevsky B and Miura RM (1986) Quantification of membrane properties of trigeminal root ganglion neurons in guinea pigs. *J Neurophysiol* **55** : 995–1016.
- 14) Puil E, Gimbarzevsky B and Spigelman I (1988) Primary involvement of K⁺ conductance in

- membrane resonance of trigeminal root ganglion neurons. *J Neurophysiol* **59** : 77–89.
- 15) Koch C (1984) Cable theory in neurons with active, linearized membranes. *Biol Cybern* **50** : 15–33.
 - 16) Hutcheon B, Miura RM and Puil E (1996) Subthreshold membrane resonance in neocortical neurons. *J Neurophysiol* **76** : 683–97.
 - 17) Kjaerulff O and Kiehn O (2001) 5-HT modulation of multiple inward rectifiers in motoneurons in intact preparations of the neonatal rat spinal cord. *J Neurophysiol* **85** : 580–93.
 - 18) Schoepp DD, Jane DE and Monn JA (1999) Pharmacological agents acting at subtypes of metabotropic glutamate receptors. *Neuropharmacol* **38** : 1431–76.
 - 19) Conn PJ and Pin JP (1997) Pharmacology and functions of metabotropic glutamate receptors. *Annu Rev Pharmacol Toxicol* **37** : 205–37.
 - 20) Schwindt PC, Spain WJ and Crill WE. (1992) Effects of intracellular calcium chelation on voltage-dependent and calcium-dependent currents in cat neocortical neurons. *Neuroscience* **47** : 571–8.
 - 21) Hagiwara N and Irisawa H (1989) Modulation by intracellular Ca^{2+} of the hyperpolarization-activated inward current in rabbit single sino-atrial node cells. *J Physiol* **409** : 121–41.
 - 22) Zaza A, Maccaferri G, Mangoni M and DiFrancesco D (1991) Intracellular calcium does not directly modulate cardiac pacemaker (If) channels. *Pflugers Arch* **419** : 662–4.
 - 23) Cardenas CG, Del Mar LP, Vysokanov AV, Arnold PB, Cardenas LM, Surmeier DJ and Scroggs RS (1999) Serotonergic modulation of hyperpolarization-activated current in acutely isolated rat dorsal root ganglion neurons. *J Physiol* **518** : 507–23.
 - 24) Gasparini S and DiFrancesco D (1999) Action of serotonin on the hyperpolarization-activated cation current (I_h) in rat CA 1 hippocampal neurons. *Eur J Neurosci* **11** : 3093–100.
 - 25) Katakura N and Chandler SH (1991) Ionophoretic analysis of the pharmacologic mechanisms responsible for initiation and modulation of trigeminal motoneuronal discharge evoked by intra-oral afferent stimulation. *Brain Res* **549** : 66–71.
 - 26) Kogo M, Funk GD and Chandler SH (1996) Rhythmical oral-motor activity recorded in an in vitro brainstem preparation. *Somatosens Mot Res* **13** : 39–48.
 - 27) Trueblood PR, Levine MS and Chandler SH (1996) Dual-component excitatory amino acid-mediated responses in trigeminal motoneurons and their modulation by serotonin in vitro. *J Neurophysiol* **76** : 2461–73.

三叉神経一次感覚ニューロンにおける内向き整流作用のグルタミン酸受容体依存性神経修飾機構

田中 晋, 安田浩一, 古澤清文

(松本歯科大学 口腔顎顔面外科学講座)

一次感覚ニューロンである三叉神経中脳路核ニューロンは、種々の神経伝達物質によりニューロンの興奮性が修飾され、運動核より出力される咀嚼や吸啜運動などの顎運動パターン形成、調節に深く関与していると考えられている。内向き整流作用は、膜電位の過分極変化に伴い活性化される h -電流 (I_h) により誘発される特性で、中脳路核ニューロンにおいても、静止膜電位の保持、スパイク発射特性調節、周波数依存性膜応答特性形成を通じてニューロンの興奮性維持に関わっているが、神経伝達物質による I_h の神経修飾機構について詳細は明らかとされていない。本研究では、新生仔ラット (P2–12) の中脳路核ニューロンより薄切脳幹スライス標本を作製し、Whole-cell patch-clamp 記録法を用いて、代謝型グルタミン酸受容体活性に伴う I_h の神経修飾機構について検討した。

グループ I, II 代謝型グルタミン酸受容体作動薬である ACPD を還流投与により, I_h の最大振幅値は濃度依存性に有意に減少した. さらに ACPD による抑制効果は特にグループ II 受容体活性に依存しており, 修飾発現に細胞内 Ca^{2+} イオン濃度上昇が関与していることが明らかとなった.

一方, 過分極電位条件下で中脳路核ニューロンにおいて特異的に観察される低周波数 (<10Hz) 依存性膜応答特性 (low-frequency resonance) についても, ACPD 投与により有意に応答特性の低下が認められた. 以上の結果より, 代謝型グルタミン酸受容体活性に伴う I_h の抑制効果は, 特定の周波数領域のシナプス入力に対する応答特性を減弱させることにより, 中脳路核ニューロンの興奮性を巧妙に調節して顎運動パターンの制御に関わっていることが推測された.